

Linearity in the response of photopolymers as optical recording media

Sergi Gallego,^{1,2,*} Andrés Marquez,^{1,2} Francisco J. Guardiola,² Marina Riquelme,² Roberto Fernández,² Inmaculada Pascual,^{2,3} and Augusto Beléndez^{1,2}

¹Departamento de Física, Ingeniería de Sistemas y Teoría de la Señal. Universidad de Alicante. Apartado 99. E-03080 Alicante, Spain

²Instituto Universitario de Física Aplicada a las Ciencias y las Tecnologías. Universidad de Alicante. Apartado 99. E-03080 Alicante, Spain

³Departamento de Óptica, Farmacología y Anatomía. Universidad de Alicante. Apartado 99. E-03080 Alicante, Spain

Tel.: + 34-96-5903400 (ext. 3327); Fax: + 34-96-5909750;

*sergi.gallego@ua.es

Abstract: Photopolymer are appealing materials for diffractive elements recording. Two of their properties when they are illuminated are useful for this goal: the relief surface changes and the refractive index modifications. To this goal the linearity in the material response is crucial to design the optimum irradiance for each element. In this paper we measured directly some parameters to know how linear is the material response, in terms of the refractive index modulation versus exposure, then we can predict the refractive index distributions during recording. We have analyzed at different recording intensities the evolution of monomer diffusion during recording for photopolymers based on PVA/Acrylamide. This model has been successfully applied to PVA/Acrylamide photopolymers to predict the transmitted diffracted orders and the agreement with experimental values has been increased.

©2013 Optical Society of America

OCIS codes: (050.2770) Diffraction and gratings; (090.0090) Holography; (090.2900) Optical storage materials.

References and links

1. J. R. Lawrence, F. T. O'Neill, and J. T. Sheridan, "Photopolymer holographic recording material," *Optik (Stuttg.)* **112**(10), 449–463 (2001).
2. T. A. Shankoff, "Phase holograms in dichromated gelatin," *Appl. Opt.* **7**(10), 2101–2105 (1968).
3. M. Lehmann, J. P. Lauer, and J. W. Goodman, "High efficiencies, low noise, and suppression of photochrome effects in bleached silver halide holography," *Appl. Opt.* **9**(8), 1948–1949 (1970).
4. P. Günter, "Holography, coherent light amplification and optical phase conjugation with photorefractive materials," *Phys. Rep.* **93**(4), 199–299 (1982).
5. M. Ortuño, S. Gallego, C. García, I. Pascual, C. Neipp, and A. Beléndez, "Holographic characteristics of an acrylamide/bisacrylamide photopolymer in 40–1000 μm thick layers," *Phys. Scr.* **118**, 66–68 (2005).
6. J. Zheng, G. Sun, Y. Jiang, T. Wang, A. Huang, Y. Zhang, P. Tang, S. Zhuang, Y. Liu, and S. Yin, "H-PDLC based waveform controllable optical choppers for FDMF microscopy," *Opt. Express* **19**(3), 2216–2224 (2011).
7. Y.-C. Su, C.-C. Chu, W.-T. Chang, and V. K. S. Hsiao, "Characterization of optically switchable holographic polymer-dispersed liquid crystal transmission gratings," *Opt. Mater.* **34**(1), 251–255 (2011).
8. I. W. Moran, A. L. Briseno, S. Loser, and K. R. Carter, "Device fabrication by easy soft imprint nanolithography," *Chem. Mater.* **20**(14), 4595–4601 (2008).
9. M. J. Swanson and G. W. Opperman, "Photochemical surface modification of polymers for improved adhesion," *J. Adhes. Sci. Technol.* **9**(3), 385–391 (1995).
10. T. Vuocolo, R. Haddad, G. A. Edwards, R. E. Lyons, N. E. Liyou, J. A. Werkmeister, J. A. M. Ramshaw, and C. M. Elvin, "A highly elastic and adhesive gelatin tissue sealant for gastrointestinal surgery and colon anastomosis," *J. Gastrointest. Surg.* **16**(4), 744–752 (2012).
11. M.-S. Weiser, F.-K. Bruder, T. Fäcke, D. Hönel, D. Jurbergs, and T. Rölle, "Self-processing, diffusion-based photopolymers for holographic applications," *Macromol. Symp.* **296**(1), 133–137 (2010).
12. M. Toishi, T. Takeda, K. Tanaka, T. Tanaka, A. Fukumoto, and K. Watanabe, "Two-dimensional simulation of holographic data storage medium for multiplexed recording," *Opt. Express* **16**(4), 2829–2839 (2008).

13. P. Wang, B. Ihas, M. Schnoes, S. Quirin, D. Beal, S. Sethachayanon, T. Trentler, M. Cole, F. Askham, D. Michaels, S. Miller, A. Hill, W. Wilson, and L. Dhar, "Photopolymer media for holographic storage at 405 nm," *Proc. SPIE* **5380**, 283–288 (2004).
14. K. Tanaka, M. Hara, K. Tokuyama, K. Hirooka, K. Ishioka, A. Fukumoto, and K. Watanabe, "Improved performance in coaxial holographic data recording," *Opt. Express* **15**(24), 16196–16209 (2007).
15. J. Kelly, M. Gleeson, C. Close, F. O'Neill, J. Sheridan, S. Gallego, and C. Neipp, "Temporal analysis of grating formation in photopolymer using the nonlocal polymerization-driven diffusion model," *Opt. Express* **13**(18), 6990–7004 (2005).
16. J. H. Kwon, H. C. Hwang, and K. C. Woo, "Analysis of temporal behavior of beams diffracted by volume gratings formed in photopolymers," *J. Opt. Soc. Am. B* **16**(10), 1651–1657 (1999).
17. C. Neipp, S. Gallego, M. Ortuño, A. Márquez, M. L. Álvarez, A. Beléndez, and I. Pascual, "First-harmonic diffusion-based model applied to a polyvinyl-alcohol–acrylamide-based photopolymer," *J. Opt. Soc. Am. B* **20**(10), 2052–2060 (2003).
18. G. Zhao and P. Mouroulis, "Diffusion model of hologram formation in dry photopolymers materials," *J. Mod. Opt.* **41**(10), 1929–1939 (1994).
19. G. Zhao and P. Mouroulis, "Second order grating formation in dry holographic photopolymers," *Opt. Commun.* **115**(5-6), 528–532 (1995).
20. J. Kelly, M. Gleeson, C. Close, F. O'Neill, J. Sheridan, S. Gallego, and C. Neipp, "Temporal analysis of grating formation in photopolymer using the nonlocal polymerization-driven diffusion model," *Opt. Express* **13**(18), 6990–7004 (2005).
21. M. R. Gleeson, S. Liu, C. E. Close, D. Sabol, and J. T. Sheridan, "Improvement of photopolymer materials for holographic data storage," *J. Mater. Sci.* **44**(22), 6090–6099 (2009).
22. C. E. Close, M. R. Gleeson, and J. T. Sheridan, "Monomer diffusion rates in photopolymer material. Part I. Low spatial frequency holographic gratings," *J. Opt. Soc. Am. B* **28**(4), 658–666 (2011).
23. M. R. Gleeson, J. V. Kelly, C. E. Close, D. Sabol, S. Liu, and J. T. Sheridan, "Modelling the photochemical effects present during holographic grating formation in photopolymer materials," *J. Appl. Phys.* **102**(2), 023108 (2007).
24. M. R. Gleeson and J. T. Sheridan, "Nonlocal photopolymerization kinetics including multiple termination mechanisms and dark reactions. Part I. Modeling," *J. Opt. Soc. Am. B* **26**(9), 1736–1745 (2009).
25. M. R. Gleeson, S. Liu, R. R. McLeod, and J. T. Sheridan, "Nonlocal photopolymerization kinetics including multiple termination mechanisms and dark reactions. Part II. Experimental validation," *J. Opt. Soc. Am. B* **26**(9), 1746–1754 (2009).
26. A. C. Sullivan, M. W. Grabowski, and R. R. McLeod, "Three-dimensional direct-write lithography into photopolymer," *Appl. Opt.* **46**(3), 295–301 (2007).
27. A. Márquez, S. Gallego, M. Ortuño, E. Fernández, M. L. Álvarez, A. Beléndez, and I. Pascual, "Generation of diffractive optical elements onto a photopolymer using a liquid crystal display," *Proc. SPIE* **7717**, 77170D, 77170D-12 (2010).
28. A. Pu, K. Curtis, and P. Psaltis, "Exposure schedule for multiplexing holograms in photopolymer films," *Opt. Eng.* **35**(10), 2824–2829 (1996).
29. H. J. Coufal, D. Psaltis, and G. T. Sincerbox, *Holographic Data Storage* (Springer-Verlag, 2000).
30. C. Neipp, A. Beléndez, J. T. Sheridan, J. V. Kelly, F. T. O'Neill, S. Gallego, M. Ortuño, and I. Pascual, "Non-local polymerization driven diffusion based model: general dependence of the polymerization rate to the exposure intensity," *Opt. Express* **11**(16), 1876–1886 (2003).
31. C. Neipp, A. Beléndez, S. Gallego, M. Ortuño, I. Pascual, and J. Sheridan, "Angular responses of the first and second diffracted orders in transmission diffraction grating recorded on photopolymer material," *Opt. Express* **11**(16), 1835–1843 (2003).
32. S. Gallego, A. Márquez, D. Méndez, S. Marini, A. Beléndez, and I. Pascual, "Spatial-phase-modulation-based study of polyvinyl-alcohol/acrylamide photopolymers in the low spatial frequency range," *Appl. Opt.* **48**(22), 4403–4413 (2009).
33. S. Gallego, A. Márquez, M. Ortuño, J. Francés, I. Pascual, and A. Beléndez, "Relief diffracted elements recorded on absorbent photopolymers," *Opt. Express* **20**(10), 11218–11231 (2012).
34. I. Pascual, A. Beléndez, F. Mateos, and A. Fimia, "Obtención de elementos ópticos holográficos con fotorresinas AZ-1350: comparación entre métodos directo y copia," *Óptica Pura y Aplicada* **24**, 63–67 (1991).
35. T. Babeva, I. Naydenova, D. Mackey, S. Martin, and V. Toal, "Two-way diffusion model for short-exposure holographic grating formation in acrylamidebased photopolymer," *J. Opt. Soc. Am. B* **27**(2), 197–203 (2010).
36. J. V. Kelly, F. T. O'Neill, C. Neipp, S. Gallego, M. Ortuño, and J. T. Sheridan, "Holographic photopolymer materials: non-local polymerisation driven diffusion under non-ideal kinetic conditions," *J. Opt. Soc. Am. B* **22**(2), 406–407 (2005).
37. S. Gallego, A. Márquez, M. Ortuño, S. Marini, and J. Francés, "High environmental compatibility photopolymers compared to PVA/AA based materials at zero spatial frequency limit," *Opt. Mater.* **33**(3), 531–537 (2011).
38. S. Gallego, A. Márquez, D. Méndez, M. Ortuño, C. Neipp, E. Fernández, I. Pascual, and A. Beléndez, "Analysis of PVA/AA based photopolymers at the zero spatial frequency limit using interferometric methods," *Appl. Opt.* **47**(14), 2557–2563 (2008).
39. P. Hariharan, "Optical Holography: principles, techniques, and applications," *Cambridge Studies in Modern Optics*, second Edition, p. 47 (1996).
40. S. Gallego, M. Ortuño, I. Pascual, C. Neipp, A. Márquez, and A. Beléndez, "Analysis of second and third diffracted orders in volume diffraction gratings recorded on photopolymers," *Phys. Scr.* **118**, 58–60 (2005).

1. Introduction

A large selection of photosensitive materials can be used to record holograms and diffractive optical elements (DOE) including photopolymers, silver halide, photorefractives, photoresins, etc [1–4]. Each one has advantages and disadvantages with respect to the others and the application dictates the choice of which one to use. Photopolymer materials enable modulation of the material's permittivity and thickness, they are self processing, layers with a wide range of thicknesses and properties can be fabricated [5–7], they present low scattering and are reasonably cheap. Altogether makes photopolymers a versatile and advantageous material. Nowadays photopolymers are optimized for many applications [8–10] and some important companies are developing different chemical variations of these materials [11–14].

Due to the photopolymers importance many attempts have been done in order to model their behavior during and after the recording process [15–17]. The simplicity of the first models [18, 19], was completed by more accurate ideas demonstrating the influence of the many parameters involved in the image formation in this type of materials, and as a consequence the various models have become more and more complex [20, 21]. For example there are many models taking a deep insight into the chemical kinetic reactions during exposure [21–25] or in the size of the polymer chains in order to predict the maximum spatial frequency that can be recorded. Recently the possibility to record phase diffractive optical elements onto photopolymers has been explored [26, 27]. Two of their properties when they are illuminated are useful to this goal: the relief surface changes and the refractive index modifications. One of the most important properties of photopolymers as a basis for diffractive optical elements is the linearity in their response during recording, in other words, the dependence of the refractive index modulation as a function of recording time or energy exposure. When the material response is linear, then the fidelity in the recording is ensured, enabling to find easily the optimum intensity distribution to obtain the desired DOE with the desired relief structure or refractive index distribution. In the case when the material presents a non-linear response, the recording intensity must be adequately modified, by means of the appropriate mapping function between phase modulation and exposure time, to obtain an optimum DOE. In addition there are applications such as in holographic data storage where the linearity in the material response is important but not dramatic [28, 29] yet it needs to be conveniently characterized.

In the literature papers can be found some where the linearity of holographic recording materials response is analyzed [30, 31]. One of these methods consists in the measurement of the second and third diffracted orders around their respective angular Bragg replay [31]. The experimental results, presented in one of these works, show the high linearity and fidelity of photopolymers based on polyvinylalcohol/acrylamide (PVA/AA) to record spatial frequencies around 1000 lines/mm even in the case when the holographic grating is overmodulated, that is the layer is in the saturated region [31].

In this paper firstly we have analyzed the importance of the material linearity in order to record DOEs, and on the second place we have checked the linearity of PVA/AA based photopolymers when thin sinusoidal gratings are recorded.

2. Theoretical and experimental development

The sinusoidal profile is the easiest profile to record in a holographic recording material. i.e. it can be obtained by the simple interference of two plane wave beams [22] or alternatively using a spatial light modulator [32, 33]. Other sharper profiles may as well present a clear smoothing of the edges due to various reasons: the cut-off frequency (a low pass filtering) of the optical system, the finite size of polymer chains, monomer diffusion, and non-linearities in the recording process. For volume holograms the existence of higher harmonics can be produced by an overexposure of the sample. In the overexposed samples the high

concentration of polymer prevents the arrival of diffused monomer to the most illuminated areas and deviations of the sinusoidal profile can be found. This is similar to the effects measured in materials without diffusion such as photoresins [34]. These deviations depend on the parameter R that indicates the relative importance of the polymerization with respect to the monomer diffusion [17, 28], and is defined as:

$$R = \frac{DK_g^2}{F_R} \quad (1)$$

Where D is the monomer diffusivity, F_R is the polymerization rate and K_g is the grating number that is related to the grating period Λ by means of $K_g = 2\pi/\Lambda$.

Other parameters that influence the linearity of the material response are the low intensity cut-off (under this cut-off intensity the material does not react), the inhibition period, and the dependence of the polymerization rate with the incident intensity. The inhibition period takes place at the start of grating growth during which the formation of polymer chains is suppressed. One way to express the dependence of the polymerization rate on the recording intensity for a sinusoidal illumination is:

$$F_R(t) = k_R(t) \cdot I^\gamma(x, z, t) = k_R \left(I_0 \left[1 + V \cos(K_g x) \right] e^{-\alpha(t)z} \right)^\gamma \quad (2)$$

where $k_R(t)$ is the polymerization parameter that depends on the chemical kinetics, $I(x, z, t)$ is the recording intensity distribution that is exponentially attenuated with the depth due to the dye's absorption (Beer's law), α indicates this absorption (decreases when the dye is consumed for the recording intensity), V is the visibility of the fringes (1 in this work) and γ indicates the relation between polymerization rate and the recording intensity. This parameter is usually between 0.5 and 1. The value of 0.5 is for more liquid polymerisable systems and 1 for more solid systems.

In the first attempts to model the photopolymers behavior carried out by Zhao and Moroulis [18,19] one of the main problems was the difficulty to fit an exact value of γ . Nowadays recent studies have proposed detailed models of the kinetics chemical reaction that takes place during recording. In this sense the accurate study of the photochemical reactions and the polymer chains growth show that after the inhibition period the polymerization parameter, k_R , decays exponentially due to the increase in the viscosity [23].

In this sense we have analyzed the effect on the parameter γ of quantities such as triethanolamine's (TEA) concentration. To obtain a first approximation to this value we have assumed a constant value of the polymerization rate and the inhibition period can be disregarded for our experiments due to the long recording times analyzed.

Three dimensional behavior of monomer and polymer volume fractions (M , and P respectively) can be described by the following general equations:

$$\frac{\partial M(x, z, t)}{\partial t} = \frac{\partial}{\partial x} D(x, z, t) \frac{\partial M(x, z, t)}{\partial x} + \frac{\partial}{\partial z} D(x, z, t) \frac{\partial M(x, z, t)}{\partial z} - F_R(x, z, t) M(x, z, t) \quad (3)$$

$$\frac{\partial P(x, z, t)}{\partial t} = F_R(x, z, t) M(x, z, t) \quad (4)$$

In Eq. (3) and (4) we have to determine the dependence of D and F_R with the variables x , z and t . The simplest approximation is to assume that these variables are constant [33], but many works have focused their efforts calculating accurately these parameters [22–25, 35]. In particular F_R has been very much studied since it includes all the chemical reactions that take place in the material during the exposure [23]. We have used the finite difference method to solve numerically the differential Eqs. (3) and (4) [20, 33]. In this paper we have assumed initially a constant value of D and we have approximated the dependence of the polymerization with the intensity only taking into account the last exponential decay of the polymerization constant with time [36], that allows us write:

$$k_r(t) = k_{r0} \exp(-\alpha_T t) \quad (5)$$

, where α_T is the attenuation of the polymerization due to the Trommsdorff's effect [36].

The volume fraction is given normally by $\phi_i = x_i v_i / \sum x_i v_i$, where x_i is the molar fraction and v_i is the molar volume of the i^{th} component [37, 38]. In order to calculate the refractive index of the layer as a function of the variations in the volume fraction of each component, we can use the Lorentz-Lorenz equation:

$$\frac{n^2 - 1}{n^2 + 2} = \frac{n_m^2 - 1}{n_m^2 + 2} M + \frac{n_p^2 - 1}{n_p^2 + 2} P + \frac{n_b^2 - 1}{n_b^2 + 2} (1 - M_0) \quad (6)$$

where M_0 is the average initial value for the volume fraction of monomer, n_p is the polymer refractive index, n_m is the monomer refractive index, n_b is the binder refractive index. The effect of holes generation and collapse described in reference [15] does not affect, thus we assume that volume fraction of holes is constant.

We believe that the study of the linearity of material response can be observed analyzing the recording process for very small spatial frequencies, generating thin diffraction gratings, due to two reasons. On the first place for volume gratings only three harmonics in the refractive index distribution can be measured for spatial frequencies around 1000 lines/mm whereas for thin gratings we obtain a good approximation of the recorded profile analyzing the Fraunhofer domain [30]. On the second place for very low spatial frequencies, in thin gratings, the monomer diffusion has less influence in the diffractive image formation; therefore we obtain larger values of the R parameter than the ones obtained for holographic regime. Therefore we are in the most non-linear case. The diffraction efficiency for the different diffracted orders in Fraunhofer domain is given by the Bessel equations [39]. In Fig. 1 we present the behavior of the four main diffraction orders for thin gratings as a function of the phase depth of the grating. The comparison of our diffraction efficiency results with this figure provides us a first approximation of the linearity of our material response.

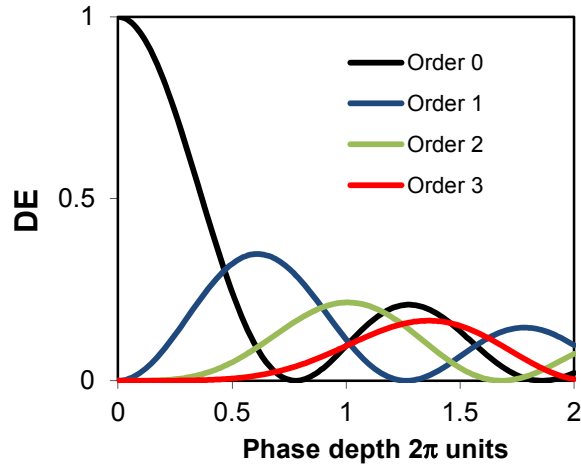


Fig. 1. Diffraction efficiency for the first four orders for a sinusoidal grating as a function of the phase depth.

In general, the composition of photopolymers includes one or more monomers, a photosensitive dye and an initiator resulting in either a liquid or a dry layer system. Dry photopolymers also usually contain a polymeric binder in addition to the other components. The material analyzed in this work is similar to the one presented in [33] using as crosslinker N, N'-Methylene-Bis-Acrylamide (BMA) (see Table 1). Moreover, different triethanolamine

(TEA) concentrations are normally used to obtain different material properties (TEA is a liquid at ambient temperature and plays an important role in the monomer and polymer diffusion during the polymerization process and in the polymerization rate too). The last component of PVA/AA standard photopolymer is the dye, Yellowish Eosin (YE), which presents good absorption at 532 nm (Nd-YVO4 laser), the recording intensity, and no absorption at 632 nm (He-Ne laser), the reading intensity. The experimental set up is the same used in [22, 37].

Table 1. Chemical composition of the water solutions

Composition type	AA (g)	BMA (g)	H ₂ O (ml)	TEA (ml)	PVA (ml) (15% w/v)	YE (0.8% w/v) (ml)
A	0.96	0.25	12.5	0.7	12.5	0.6
B	0.96	0.25	12.5	1.1	12.5	0.6
C	0.96	0.25	12.5	2.3	12.5	0.6

3. Results and discussion

We have divided this section in different subsections in order to analyze the different aspects that are involved in the linearity response of the material. Firstly we have analyzed the influence of γ parameter, the general dependence of the polymerization rate with the exposure intensity. In this sense we have also simulated the behavior of the material response for different values of parameter R. On the last part we have carried out some experiment to analyze the influence of chemical composition on the monomer diffusion during exposure and on the magnitude of the parameter γ using photopolymers based on PVA/Acrylamide.

3.1. Dependency of polymerization rate with recording intensity

In this section we want to check the effects of γ in the values of the main diffracted orders for very low spatial frequencies. As we have commented this value governs in a first approximation the linearity in the material response and is fitted between 0.5 for liquid systems and 1 for more solid photopolymers.

We have run a series of simulations to study the behavior of the first four diffracted orders as a function of time for the values of γ : 0.5, 0.7, 0.9 and 1 for PVA/AA based photopolymers. The values used in our simulation are similar to the ones used in [22] which were fitted using direct methods for PVA/AA based materials [37]. We consider a thickness of 120 μm , and the other parameters introduced were taken from the “zero spatial frequency” analysis $D_m = 1.5 \mu\text{m}^2/\text{s}$; polymerization constant $k_R = 0.007 \text{ cm}^{2\gamma}/(\text{s}\cdot\text{mW}^\gamma)$, $\alpha_T = 0.004 \text{ s}^{-1}$, attenuation of light inside the material $\alpha = 0.02 \mu\text{m}^{-1}$, $M_0 = 0.22$ volume fraction, recording intensity $I_0 = 0.5 \text{ mW}/\text{cm}^2$, $n_m = 1.486$, $n_b = 1.474$; $n_p = 1.537$ and $n_{\text{dark}} = 1.478$. The results are presented in Fig. 2. In Fig. 2(a) we see that at about 60 s of exposure clear deviations appear with respect to Fig. 1 (sinusoidal grating) due to the low value of γ . These deviations increase with the exposure as expected. In the following figures the similitude with the sinusoidal grating increase with γ value as expected. There are many techniques to analyze the deviation in the recorded profile from the sinusoidal, such as the measurement of the higher harmonics in the refractive index profile distribution. Nevertheless the main advantage of the very small spatial frequencies is that the differences between two profiles can be detected directly just analyzing the different diffraction efficiencies of the different orders. To analyze the fidelity of the recording the case of sinusoidal grating Fig. 1 can be compared to Fig. 2. In Fig. 1, sinusoidal case, we observe that the efficiency of zero order drops to zero when the phase depth is about $0.7 \times 2\pi$ radians. In this sense when the diffraction efficiency of the zero order does not achieve this zero value we can conclude that the recorded grating is not sinusoidal.

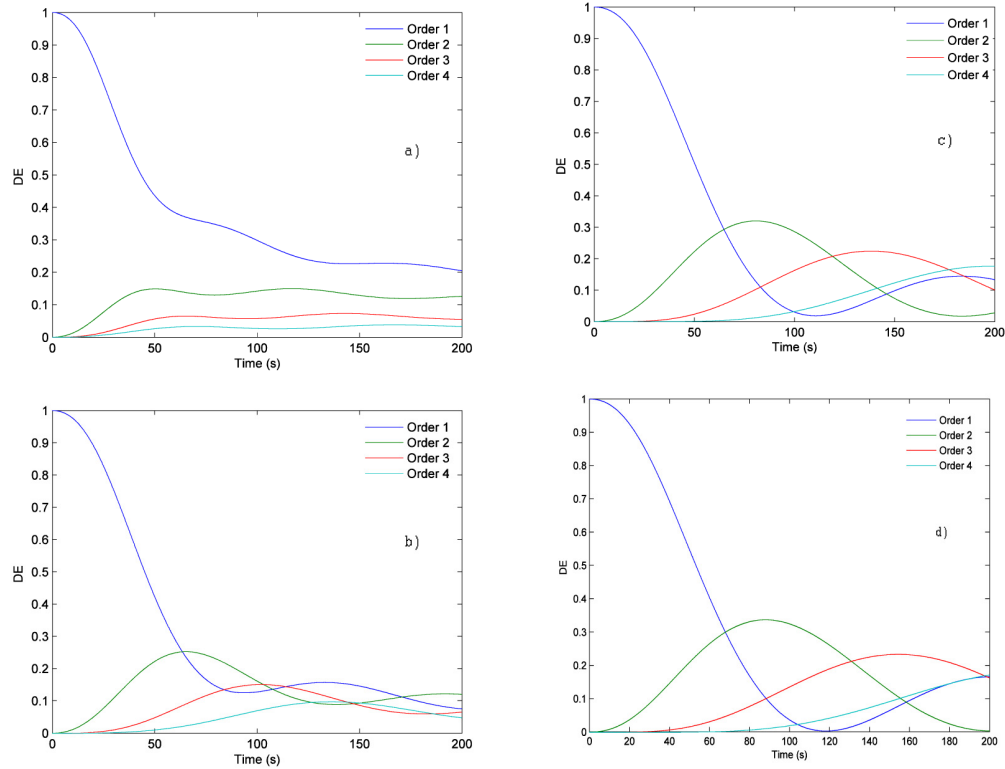


Fig. 2. Diffraction efficiency of the four first orders obtained by the simulations using the model for different values of γ . a) $\gamma = 0.5$, b) $\gamma = 0.7$, c) $\gamma = 0.9$ and d) $\gamma = 1$.

To obtain a numerical value of γ we follow the same deductions of [37]. We assume an exponential decrease of M , which is proportional to the creation of P , therefore we can fit the equation for each exposure intensity:

$$\ln\left(1 - \frac{PS}{PS_{\infty}}\right) = -I'K_R t = -F_R t \quad (7)$$

We have analyzed the results on the material for three different recording intensities in order to apply Eq. (7) using the zero spatial frequency analysis [37]. Applying this approach we illuminate an area of 1cm^2 of material and using interferometric methods we can measure the phase shift (PS) between exposed and non-exposed zones as a function of time without the diffusion influence. Once the chemical reaction stops the PS remains constant and this is the saturation regime. In Fig. 3 we present the phase shift in transmission for three different incident intensities over a sample $90\ \mu\text{m}$ thick. As it can be seen in this figure, for our samples the lowest intensity presents the best energetic sensitivity. This fact indicates that γ is smaller than 1.

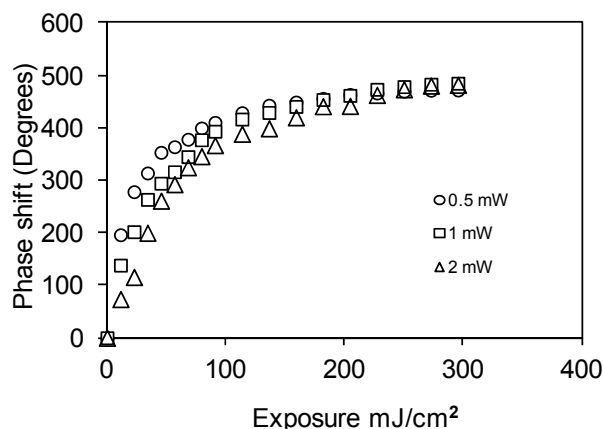


Fig. 3. Phase shift as a function of exposure for different intensities for chemical composition B.

The experimental results for three compositions are presented in Table 2 for the three intensities 0.5 mW, 1 mW and 2 mW. The values of F_R decrease when the concentration of TEA is increased. Since we assume that the value of K_R is equal in the three cases, comparing the three values of F_R obtained and using Eq. (7) we obtain three values of γ , one for each composition: 0.5 mW with 1 mW, 0.5 with 1 mW and 1mW with 2 mW.. Nevertheless the expected decrease of γ for high concentrations of TEA is very weak. In any case these results agree with previous studies focused on similar materials where the consideration of $\gamma = 1$ reported good prediction for different values of the recording intensity [17].

Table 2. Fitted values of F_R

Intensity mW	0.5	1	2	$\gamma_{0.5-1}$	$\gamma_{0.5-2}$	γ_{1-2}
A	$F_R = 0.0077 s^{-1}$	$F_R = 0.0145 s^{-1}$	$F_R = 0.0265 s^{-1}$	0.90	0.90	0.88
B	$F_R = 0.0059 s^{-1}$	$F_R = 0.0110 s^{-1}$	$F_R = 0.0205 s^{-1}$	0.90	0.88	0.86
C	$F_R = 0.0043 s^{-1}$	$F_R = 0.0076 s^{-1}$	$F_R = 0.0141 s^{-1}$	0.82	0.88	0.82

3.2. Relation between monomer diffusion and diffusivity

Using the earlier photopolymer compositions the discussion of the preponderance between diffusion and polymerization has been presented. When analyzing the recording of volume holograms only indirect observations of the process involved in the hologram formation can be done. Diffusion has been sometimes disregarded in these materials, maybe due to the very fast stabilization of the hologram after exposure, which when not appropriately monitored may lead the authors to think that the movement of the particles inside the material is not important. Recent studies show the importance of diffusion inside the hologram. Parameter R is the one showing the importance of polymerization and diffusion in the phase image formation in photopolymers. In general, values of $R \sim 0.01$ show the polymerization predominance and values of $R > 10$ indicate that diffusion dominates [17].

In Fig. 4 we have simulated the behavior during recording for different values of R . In particular we have examined the importance of the recording intensity for a material with $n_p = 1.51$, $\Lambda = 168 \mu\text{m}$, $D_0 = 1.5 \mu\text{m}^2/\text{s}$, $\alpha_T = 0.008 s^{-1}$, $\alpha = 0.02 \mu\text{m}^{-1}$, $\gamma = 1$ and $K_R = 0.0032$ for recording intensities of 1, 2 and 5 mW/cm², in other words $R = 0.066$, 0.033 and 0.013 respectively. These cases are close to the regime when polymerization becomes predominant, therefore saturation is induced and the recorded profile should not be sinusoidal. This prediction is well supported by the results presented in Fig. 4. For $R = 0.066$, Fig. 4(a), we still obtain a sinusoidal profile after 200s. For $R = 0.033$, Fig. 4(b), some small deviations

from the sinusoidal profile can be observed after 90 s. and for $R = 0.011$, Fig. 4(c), the deviations appear before 50 s and from this moment the differences between the recorded profile and the exposure pattern increase dramatically. As a summary we have shown that to obtain a higher linearity in the material refractive index modulation weak intensities are required.

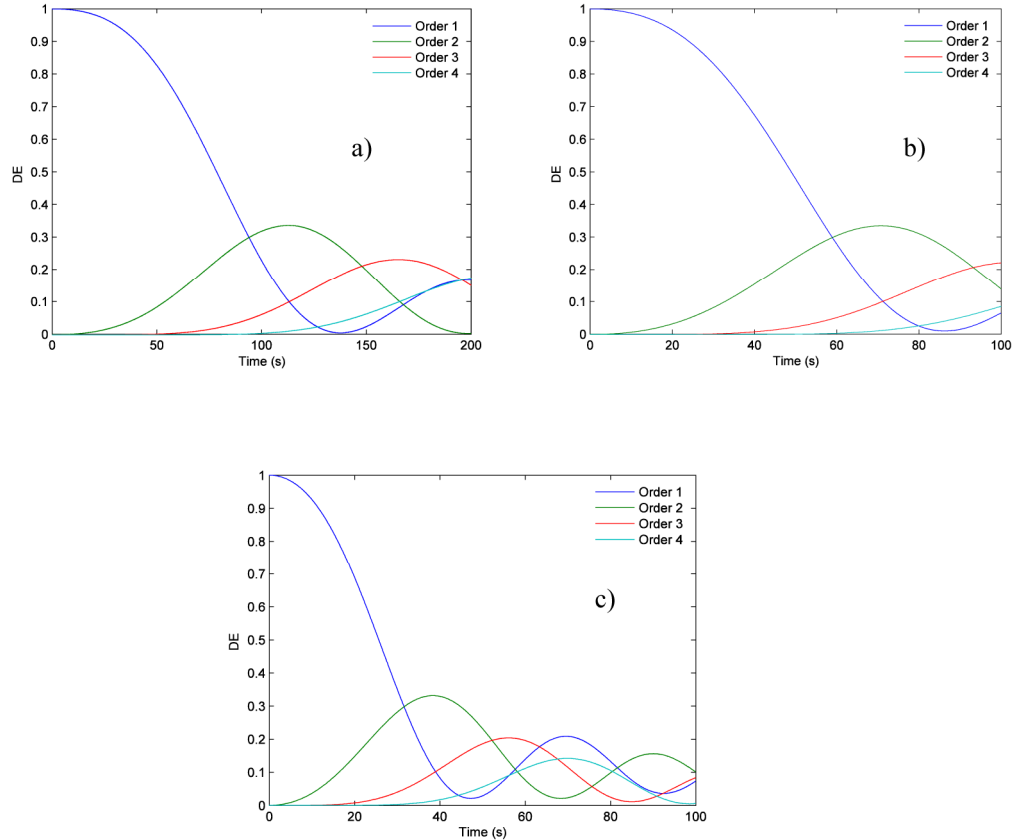


Fig. 4. Simulations of the main four orders for different recording intensities. a) $I = 1$ mW/cm^2 , b) $I = 2$ mW/cm^2 c) $I = 5$ mW/cm^2

In addition to the recording intensity another important parameter influencing material linearity is the monomer diffusion. To have a deep insight in this aspect we have simulated the response of two materials with $D_0 = 1.5 \mu\text{m}^2/\text{s}$ (Fig. 5.a) and $D_0 = 0.15 \mu\text{m}^2/\text{s}$ (Fig. 5(b)) and identical in the rest of parameters $n_p = 1.51$, $\Lambda = 168 \mu\text{m}$, $\gamma = 1$, $Kr = 0.007$ $I = 10$ mW/cm^2 . Therefore the values of R are 0.003 and 0.0003. In Fig. 5(a) deviations from the sinusoidal profile are small, as in Fig. 4. On the contrary we observe huge deviations from the sinusoidal profile in Fig. 5(b). It is important to note that the deviations due to the low values of R may be desirable in some applications, such as to obtain saturated thin gratings with higher values of the first diffracted order than sinusoidal ones. This type of results is used in optical recording materials like photoresists where diffusion does not take place. In this case using a sinusoidal recording intensity distribution it is possible to obtain gratings with 40% of diffraction efficiency because the recorded profile is sharper than the sinusoidal.

These results are in agreement with the holographic case i.e. high spatial frequencies and volume regime, in similar materials where the second and third harmonics in the recorded profile were lower than 1/8 and 1/14 respectively. It is important to note that in this case the spatial frequency was 1125 lines/mm and consequently the value of R was clearly larger [40].

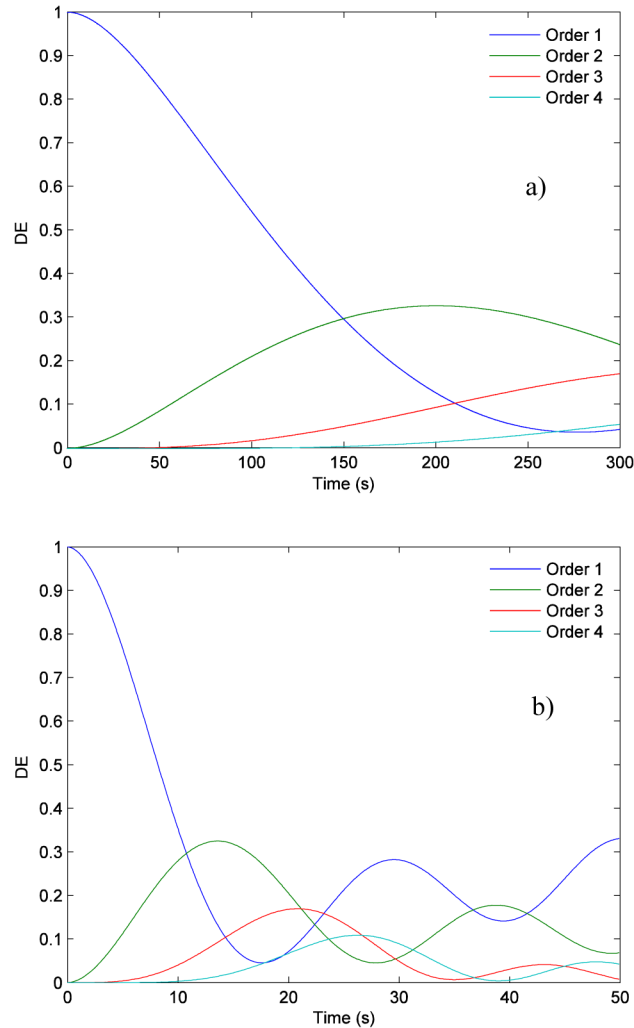


Fig. 5. Simulations of the main four orders for different values of D . a) $D = 1.5 \mu\text{m}^2/\text{s}$, b) $D = 0.15 \mu\text{m}^2/\text{s}$.

In order to obtain good information about the exact value and evolution of the monomer diffusion it is important to analyze the dependence of the monomer diffusion on the average polymer concentration or exposure time. It is well known that the generation of the chains of polymer difficult the movement of monomer molecules, in other words, decrease the monomer diffusion inside the material. In a previous examination of a similar model applied to the prediction of the relief structure generated in the material during and after recording [22], the assumption of a constant value of monomer diffusion only permitted to predict the correct evolution of the material in an interval between 50 and 80 s with recording intensity of $0.5 \text{ mW}/\text{cm}^2$. To increase the accuracy of the diffusion model in [22] it was proposed as a future task to take into account changes in the monomer diffusion. Therefore to confirm or refuse this idea we have measured the monomer diffusion for different polymer concentrations. Using the method applied in ref [41] we have measured the evolution of the grating after recording. We use diffractive methods [41] to obtain the refractive index modulation for some different times after the recording, $\Delta n(t)$, and the final refractive index modulation when the post recording evolution stops, $\Delta n(\infty)$. We have measured the monomer diffusion for the layer of chemical composition B after four different exposure times 16, 30,

100 and 200 s, and the fittings are plotted in Fig. 6. The recording pattern used is a sinusoidal pattern with spatial period of 168 μm and amplitude of 0.5 mW/cm^2 . As it can be seen the value of the slope decreases with the exposure time as we expected.

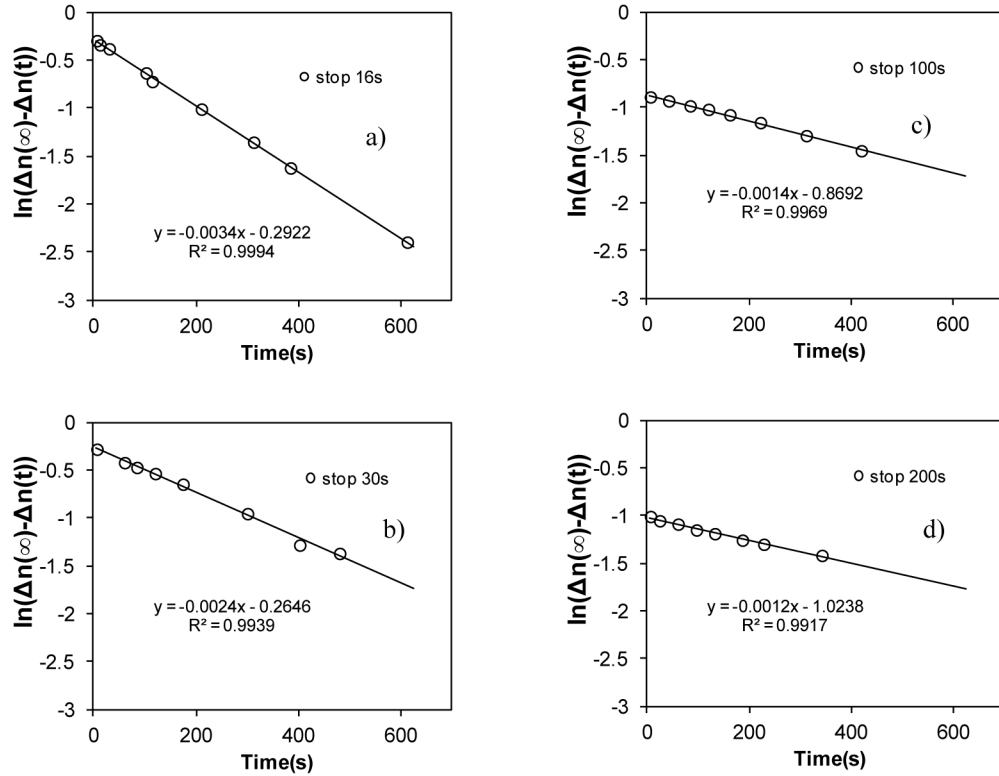


Fig. 6. Fittings to obtain D for different exposure time values. a) 16s, b) 32s, c) 50s d) 100s.

The experimental results for monomer diffusion obtained from the fittings are represented in Fig. 7. It can be seen an initial fast decrease in the monomer diffusion and later this value tends asymptotically to a constant value. In order to obtain a first approximation of the monomer diffusion variation as a function of time, to be introduced in the diffusion model, we have used the following Eq. (8) to minimize the quadratic difference between the values reported by Eq. (8) with respect to the experimental points.

$$D = D_{\infty} \left[(D_0 - 1) e^{(-\alpha_D t)} - 1 \right] \quad (8)$$

Where D_0 is the initial value of monomer diffusion, before recording, the D_{∞} is the asymptotic value of monomer diffusion when all the monomer is polymerized. The values of the parameters fitted are $D_0 = 3 \mu\text{m}^2/\text{s}$, $D_{\infty} = 0.78 \mu\text{m}^2/\text{s}$, $\alpha_D = 0.025\text{s}^{-1}$, and the experimental data and the fitting are represented in Fig. 7. This decrease should be more significant for holographic spatial frequencies where the diffusion is faster, the polymerization density larger and the increase in the material viscosity too.

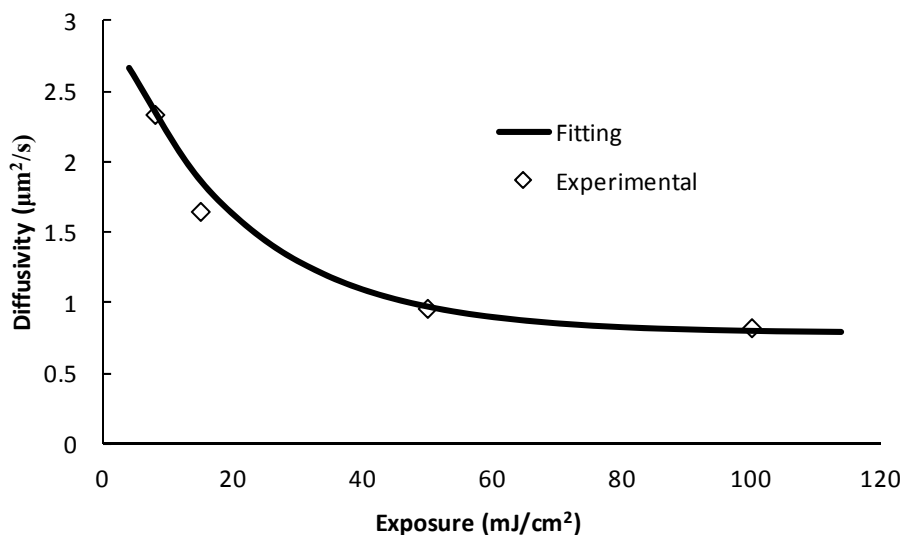


Fig. 7. Experimental values of monomer diffusion as a function of exposure and the fitting using Eq. (8).

In order to analyze the influence of the varying monomer diffusion incorporated in the diffusion model we have compared the prediction of the model with the measured experimental results obtained in the recording of a grating with spatial period of $168 \mu\text{m}$. The parameters used in the model are extracted from the zero frequency analysis for chemical composition B and are $n_p = 1.517$, $\Lambda = 168 \mu\text{m}$, $D_0 = 3 \mu\text{m}^2/\text{s}$, $D_\infty = 0.78 \mu\text{m}^2/\text{s}$, $\alpha_D = 0.025\text{s}^{-1}$, $\gamma = 0.9$ and $Kr = 0.011 (\text{cm}^2/\text{mW})^{0.9}$, $\alpha_T = 0.005 \text{s}^{-1}$, thickness $d = 120 \mu\text{m}$ and recording intensity of $0.5 \text{mW}/\text{cm}^2$. These results are represented in Fig. 8. There we see that the range of validity of the prediction of the model is increased from 70s to about 140s. This enables this model to predict the behavior in transmission for different diffractive elements recorded onto photopolymers based in PVA/AA. On the other hand we can say that probably the model can be improved using more accurate description of the polymerization rate. In this sense, parameters such as the dye concentration, temperature, humidity may have influence. In Fig. 8(b) we represented the results provided with the model when a constant value of $D = 1.5 \mu\text{m}^2/\text{s}$ was taken into account. In this Fig. 8(b) it can be seen the fast deviation from the experimental values and comparing with the previous figure the improvement obtained is clearly remarkable.

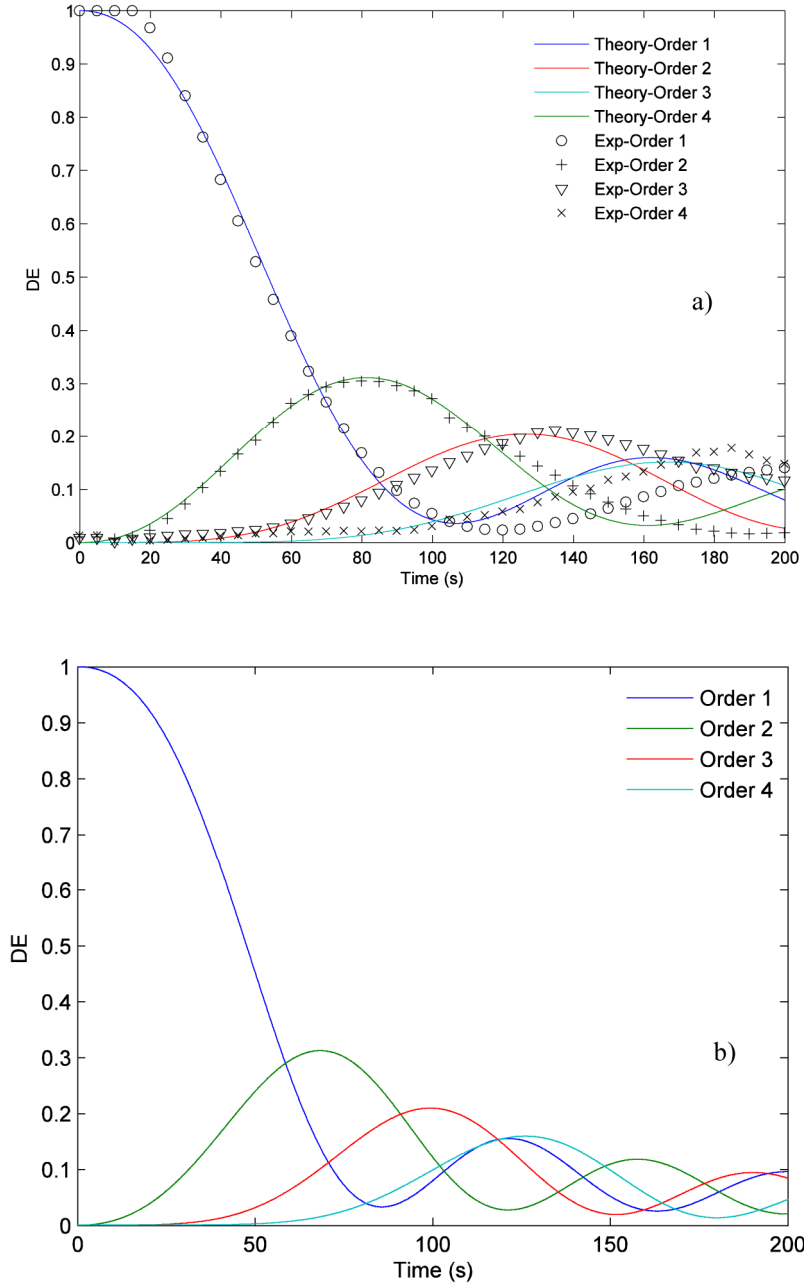


Fig. 8. - Simulations of the four main orders. a) Taking into account Eq. (8) together with the experimental results for chemical composition B, b) With constant value of monomer diffusion. For a grating with spatial period of 168 μm and sinusoidal intensity distribution.

4. Conclusions

We have focused our attention in the variation of refractive index as a function of exposure time to evaluate the fidelity of the response of photopolymers. This property is crucial in order to apply photopolymers as optical recording materials. We have shown a method to measure the linearity in the refractive index modulation with exposure at very small spatial frequencies recording a sinusoidal grating. In addition we have demonstrated the usefulness

of these measurements in order to model the recording of DOEs in these promising materials. To obtain a linear response the monomer diffusion plays an important role; therefore we have measured how this parameter changes during recording to increase the accuracy of the model. Taking into account these new parameters we have increased twofold the time interval where the model predicts the DOEs recording.

Acknowledgments

This work was supported by the Ministerio de Economía y Competitividad of Spain under projects FIS2011-29803-C02-01 and FIS2011-29803-C02-02 and by the Generalitat Valenciana of Spain under project PROMETEO/2011/021 and ISIC/2012/013.